



17th European Conference on Applied Superconductivity
21-25 September 2025, Porto, Portugal

Superconducting Digital Electronics: Current Advances and the Beginning of a New Era

Nobuyuki Yoshikawa

Yokohama National University, Japan



Outline

- Background and motivation
- Introduction to superconducting digital electronics (SDE)
 - Single flux quantum (SFQ) logic
 - Adiabatic quantum flux parametron (AQFP) logic
- Recent advancements in SDE
- New research activities in SDE
- Challenge in SDE
- Conclusions

Background

Estimated power consumption to achieve 10 exa-scale computing



~ 100 MW ~ \$100 million per year

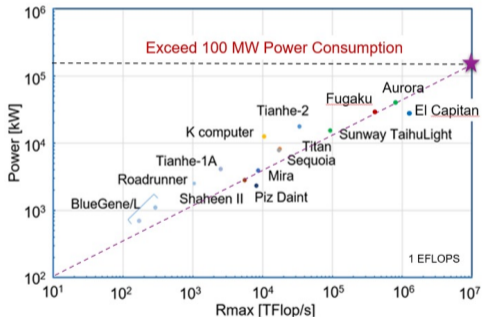
Fugaku (Japan)

Peak performance: 513 PFLOPS

Power consumption: 28.3 MW



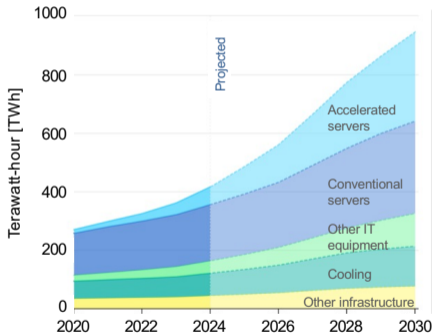
1st-ranked computers in recent TOP500



<http://www.top500.org/>

YNU YOKOHAMA National University

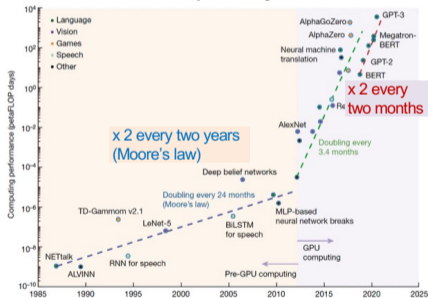
Global Data Center Electricity Consumption



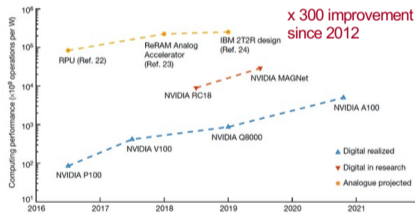
- Global electricity demand from data centers is projected to more than **double by 2030**, reaching **~945 TWh**.
- This demand is equivalent to **Japan's entire electricity consumption today**.
- **AI is the primary driver** of this rapid growth.

Computing Power Demand and Hardware Efficiency

Computing Power demand over the past 40 years

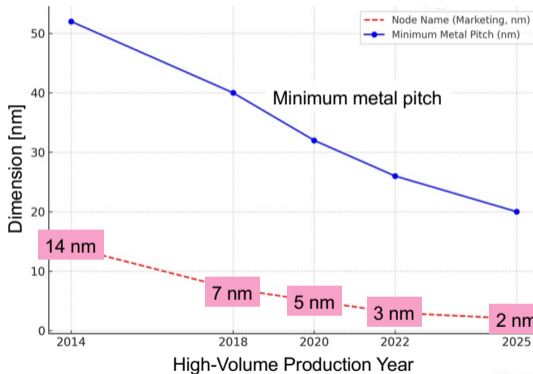


AI hardware efficiency over the past five years



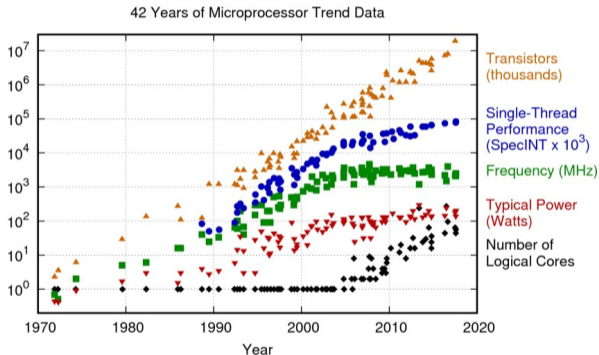
Mehonic, A., Kenyon, A.J. Brain-inspired computing needs a master plan. *Nature* **604**, 255–260 (2022).

Technology Node vs. Minimum Metal Pitch



There is a large **discrepancy** between technology **node names** and the actual **minimum metal pitch**!

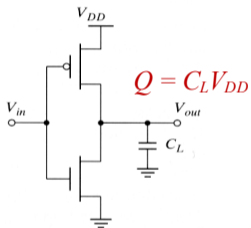
End of the Moore's Law



Original data up to the year 2010 collected and plotted by M. Horowitz, F. Labonte, O. Shacham, K. Olukotun, L. Hammond, and C. Batten
New plot and data collected for 2010-2017 by K. Rupp

Single-Flux-Quantum (SFQ) Circuits

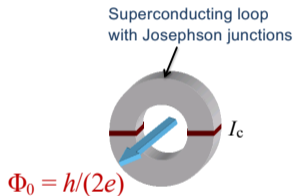
CMOS circuits



Switching energy

$$E = QV_{DD} \sim 10^{-16} \text{ J}$$

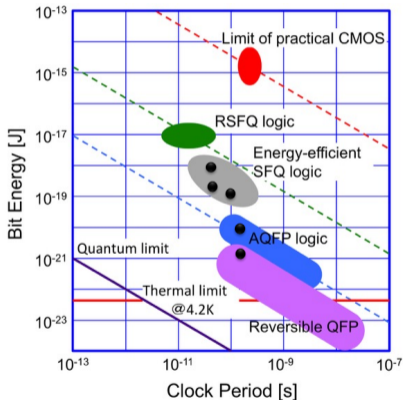
SFQ circuits



Switching energy

$$E = \Phi_0 I_c \sim 10^{-19} \text{ J}$$

Energy and Delay of Superconductor Logic



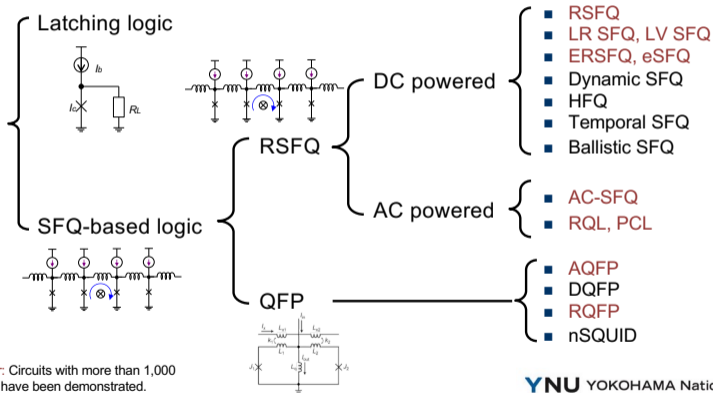
Quantum limit

$$\Delta E \Delta \tau \sim h$$

Thermal limit (Landauer's limit)

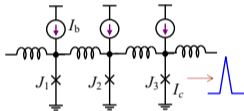
$$E \sim k_B T \ln 2$$

Classification of Josephson Logic



Superconducting Digital Logic

Rapid single-flux-quantum (RSFQ) logic and its energy-efficient variants



- DC Powered
- Operating speed \rightarrow very fast
 $f_{\text{clock}} \sim 50 - 100 \text{ GHz}$
- Switching energy \rightarrow small
 $E_b \sim I_c \Phi_0 \sim 100 k_B T$

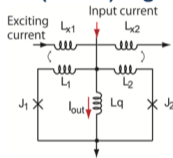
RSFQ: K. Likharev *et al.* *IEEE Trans. Appl. Supercond.* 1, 3 (1991).

ERSFQ: O. A. Mukhanov, *IEEE Trans. Appl. Supercond.* 21, 760 (2011).

eSFQ: M. Volkmann *et al.*, *Supercond. Sci. Technol.* 26, 015002 (2013).

LVSFQ: M. Tanaka *et al.*, *IEEE Trans. Appl. Supercond.* 23, 1701104 (2013).

Adiabatic quantum flux parametron (AQFP) logic

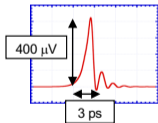
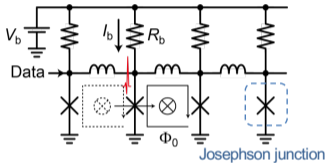


- AC Powered
- Operating speed \rightarrow fast
 $f_{\text{clock}} \sim 5 - 10 \text{ GHz}$
- Switching energy \rightarrow very small
 $E_b \ll I_c \Phi_0 \sim k_B T$

QFP: K. Loc, E. Goto, *IEEE Trans. Magn.* 21, 884 (1985).

AQFP: N. Takeuchi, *et al.*, *SUST*, 26, 035010 (2013).

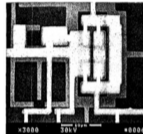
Rapid Single-Flux-Quantum (RSFQ) Logic



- Pulse height $\sim 400 \mu\text{V}$
- Pulse width $\sim 3 \text{ ps}$
- Power $\sim \text{nW/gate}$

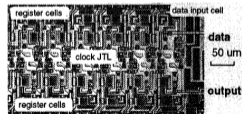
K. K. Likharev, V. K. Semenov, *IEEE Trans. Appl. Supercond.* 1, 3–28 (1991).

T Flip-flop operating at up to 770 GHz.



W. Chen *et al.*, *IEEE Trans. Appl. Supercond.* 9, 3212–3215 (1999).

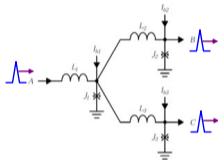
256-b shift register operating at 12 GHz



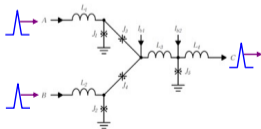
O. Mukhanov *et al.*, *IEEE Trans. Appl. Supercond.* 3, 2578–2581 (1993).

Basic Logic Components in RSFQ

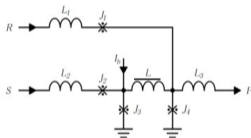
Splitter



Confluence buffer

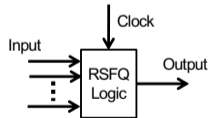
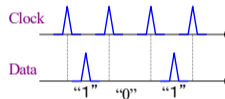


D flip-flop (DFF)

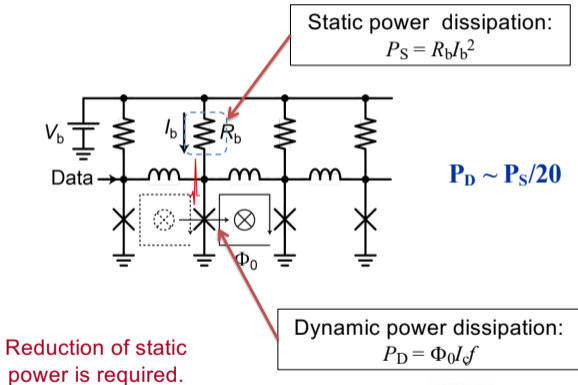


$$I_c L > \Phi_0$$

Representation of Logical States in RSFQ Logic

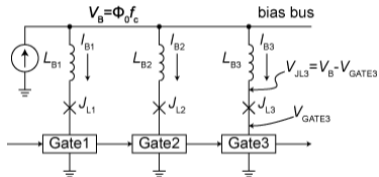


Power Consumption in RSFQ Logic



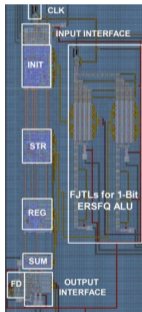
Energy-Efficient RSFQ (ERSFQ) Logic

- Bias resistors are replaced with inductors and Josephson junctions.
- A feeding JTL is required, which introduces additional switching energy.



$$P_S \sim P_D \sim I_c \Phi_0 f$$

Demonstration of ERSFQ Arithmetic Logic Unit



- Fabrication process: MIT-LL 100 $\mu\text{A}/\mu\text{m}^2$ SFQ5ee
- Maximum operating speed: 30 GHz
- Total bias current: ~ 400 mA

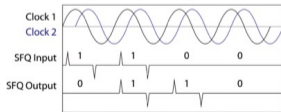
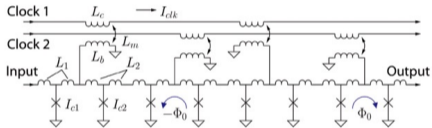
A. Inamdar et al., *IEEE Trans. Appl. Supercond.* **33**, 1300908 (2023).

Hypres O. A. Mukhanov, *IEEE Trans. Appl. Supercond.* **21**, 760 (2011).

YNU YOKOHAMA National University

Reciprocal Quantum Logic (RQL)

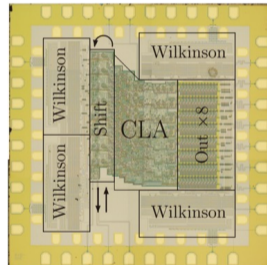
- A 4-phase AC bias current propagates digital “1” as pairs of SFQ pulses with opposite polarity.
- Gates can be biased in series.



$$P_S \sim 0,$$

$$P_D \sim I_c \Phi_0 f$$

Demonstration of 8-bit carry look-ahead adder at 10 GHz

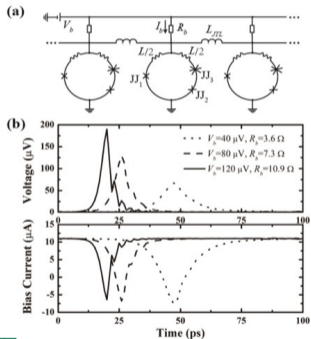


- Fabrication process: Hypres 2 um Nb process
- Power dissipation: 510 nW at 6.2 GHz

A. P. Herr *et al.*, *J. Appl. Phys.* **113**, 033911 (2013).

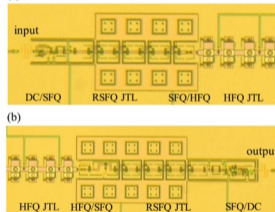
Half Flux Quantum (HFQ) Logic

HFQ JTL



- A SQUID with a π junction is used to reduce the effective critical current.
- A half flux quantum propagates in the HFQ JTL.
- Reduced energy consumption is expected.

(a) Demonstration of HFQ JTL



D. Hasegawa *et al.*, *IEEE Trans. Appl. Supercond.* 31, 1101504, 2021.

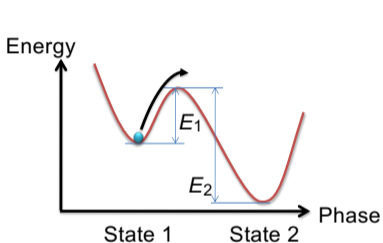
YNU YOKOHAMA National University



NAGOYA UNIVERSITY

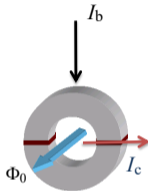
F. Li, *et al.*, *Supercond. Sci. Technol.* 34, 025013, 2021.

Energy Potential of RSFQ Logic



Input energy: E_1
 Output energy: E_2

Energy dissipation: E_2

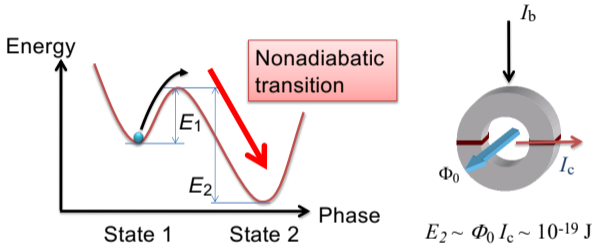


$$E_2 \sim \Phi_0 I_c \sim 10^{-19} \text{ J}$$

Requirement for the reduction of
 switching errors

$$E_1 > 100 k_B T$$

Energy Potential of RSFQ Logic



Input energy: E_1

Output energy: E_2

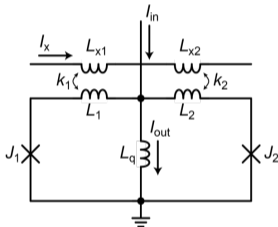
Energy dissipation: E_2

Requirement for the reduction of switching errors

$$E_1 > 100 k_B T$$

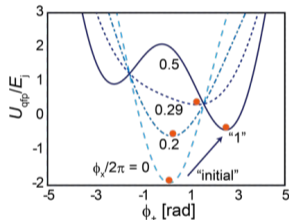
Adiabatic Quantum Flux Parametron (AQFP) Logic

AQFP gate



An SFQ is stored in the right or left loop depending on I_{in} .

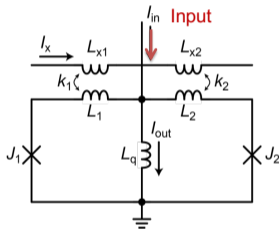
Potential energy of the gate



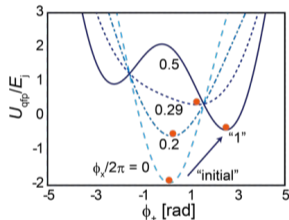
Potential energy changes adiabatically during switching.

Operation Principle of AQFP Logic

AQFP gate

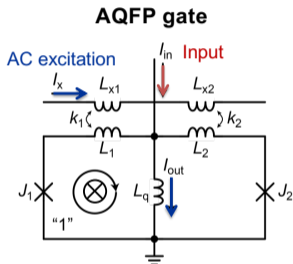


Potential energy of the gate



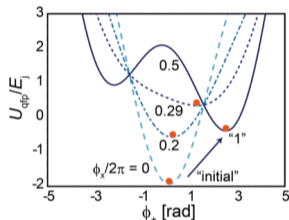
Potential energy changes adiabatically during switching.

Operation Principle of AQFP Logic



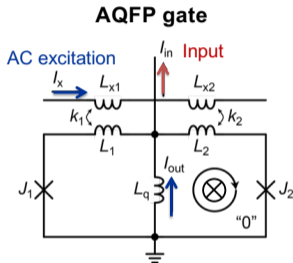
I_{out} flows downward.

Potential energy of the gate



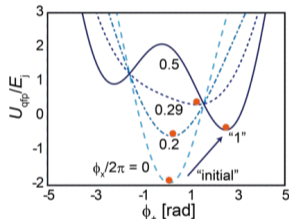
Potential energy changes adiabatically during switching.

Operation Principle of AQFP Logic



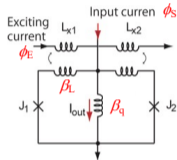
I_{out} flows upward.

Potential energy of the gate



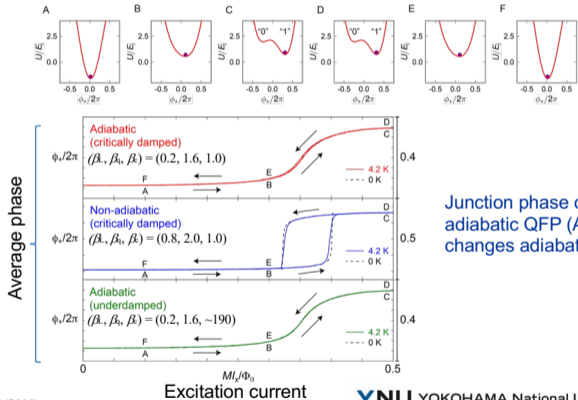
Potential energy changes adiabatically during switching.

Junction Phase vs. Excitation Current of QFP



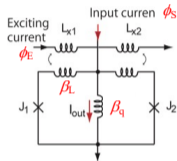
- β_C : McCumber parameter

$$\beta_C = \frac{\omega_C C}{G}$$



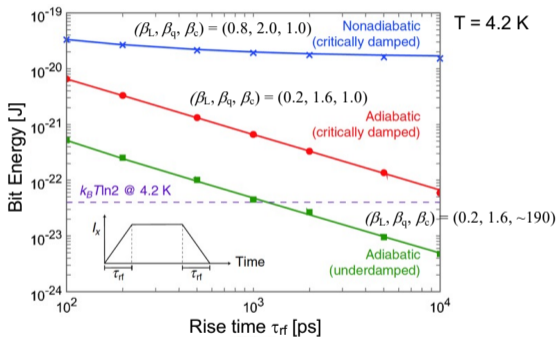
Junction phase of adiabatic QFP (AQFP) changes adiabatically.

Bit Energy vs. Rise Time of Excitation Current of AQFP



- β_c : McCumber parameter

$$\beta_c = \frac{\omega_c C}{G}$$

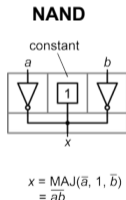
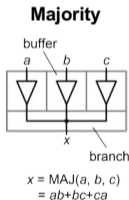
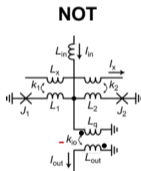
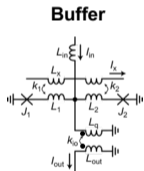
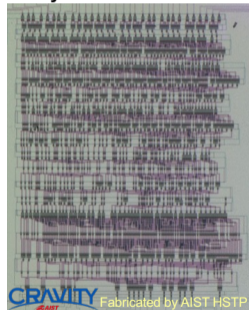


$E_{\text{bit}} \sim 0.05 \text{ zJ} (\sim k_B T)$ when rise time = 1000 ps

Design of AQFP Logic

- NOT gate is cost free.
- Majority gate is a basic logic gate.

Demonstration of AQFP 16b Carry Look-Ahead Adder



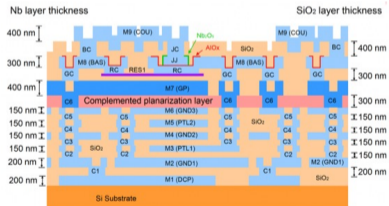
Outline

- Background and motivation
- Introduction to superconducting digital electronics (SDE)
 - Single flux quantum (SFQ) logic
 - Adiabatic quantum flux parametron (AQFP) logic
- Recent advancements in SDE
- New research activities in SDE
- Challenge in SDE
- Conclusions

Development of Process Technologies

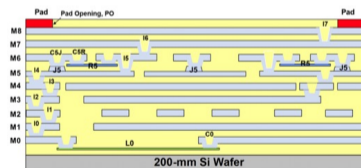
- Multilayer Nb-based Josephson IC processes have been developed worldwide, including in Japan, the United States, Germany, and China.
- Most use Nb/Al-AIOx/Nb junctions with J_c ranging 1-10k A/cm².

AIST-Qufab Nb 9-layer Advanced Process



MIT LL SFQ5ee+ Josephson Process

8-metal-layer Nb/AlOx/Nb 10-kA/cm² Josephson process

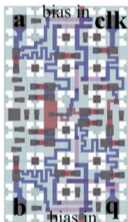


Josephson circuits with ~10k-scale are available in these processes.

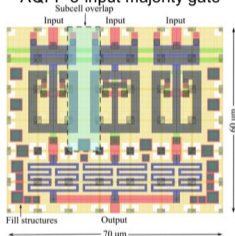
Results from the ColdFlux Project

Cell layouts using MIT LL SFQ5ee process

RSFQ 2-input OR gate

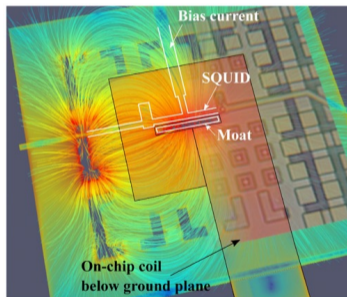


AQFP 3-input majority gate



- A parameterized cell design approach is employed.
- Layouts use a 10 x 10 μm track block, enabling SFQ-AQFP hybrid systems.

Magnetic field created by a trapped fluxon

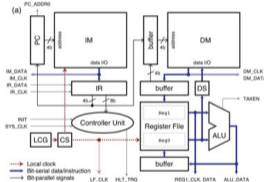


Simulated by InductEX

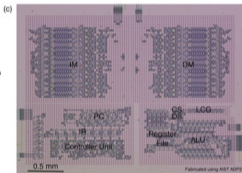
Demonstration of an RSFQ Microprocessor

An RSFQ bit-serial 8-bit microprocessor with SFQ memories is operated at 60 GHz.

Block diagram

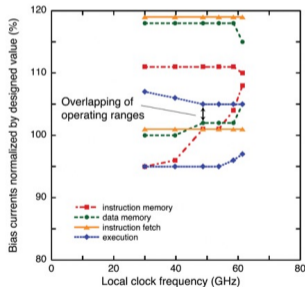


Die photo



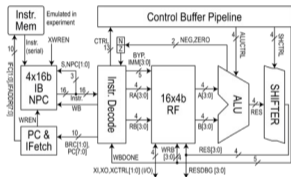
- Fabrication process: AIST 10-kA/cm² 9-Nb-layer process (ADP)
- Total junctions: 11,000 JJ
- Memory size: 256 bits, Instructions: 13
- Maximum clock frequency: 60 GHz
- Power consumption: 2.5 mW

Bias margins vs. clock frequencies

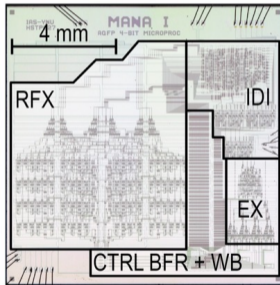


Demonstration of AQFP 4b RISC Microprocessor

MANA – Monolithic Adiabatic Integration Architecture

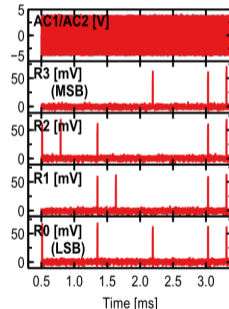


- RISC + dataflow (4-bit data, 16-bit instruction)
- 15 aJ/op @ 5GHz
- 27 cycles/operation (5.4ns @ 5GHz)
- Nb/AlOx/Nb 10 kA/cm² AIST HSTP process
- 21,460 JJs on 1 x 1 cm² chip



Execution of Test Program: add/sub + branch

(a) Full-waveform [0.5 ms to 3.4 ms]

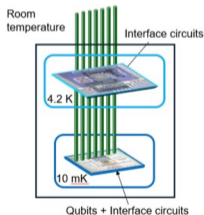
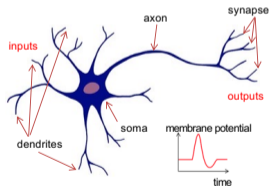


Outline

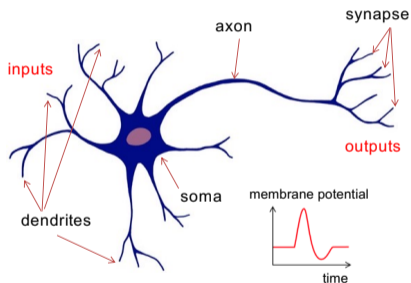
- Background and motivation
- Introduction to superconducting digital electronics (SDE)
 - Single flux quantum (SFQ) logic
 - Adiabatic quantum flux parametron (AQFP) logic
- Recent advancements in SDE
- **New research activities in SDE**
- Challenge in SDE
- Conclusions

New Research Activities in SDE

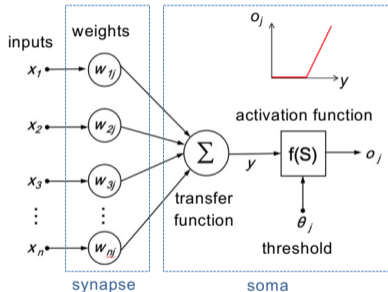
- Neuromorphic computing
- Interface with quantum computers
- Reversible computing



Neuromorphic Computing



Biological neuron



Artificial neuron model

Advantages of Neuromorphic Computing

■ Massive Parallelism

Enables efficient large-scale data processing.

■ Memory–Computation Integration

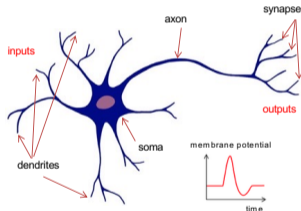
Synapses combine storage and processing, eliminating the von Neumann bottleneck.

■ Event-Driven Operation

Circuits are activated only when spikes occur, reducing power consumption.

■ Scalability

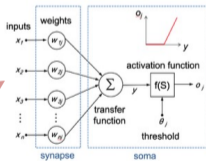
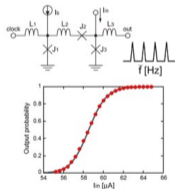
System performance improves simply by adding more neurons and synapses.



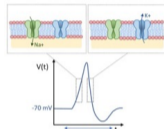
Josephson-Based Spiking Neurons

- Intrinsic spiking behavior (compact circuits)
- Ultra-fast operation (~10-100 GHz firing rates)
- Ultra-low energy consumption (~aJ per spike)

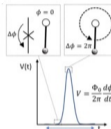
Superconducting synapse



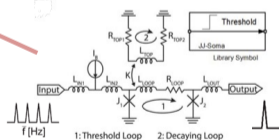
Biological action potential



SFQ pulse



Superconducting soma



A. Bozbey *et al.*, arXiv:1812.10354, 2018

M. Schneider *et al.*, *Supercond. Sci. Technol.* **35** 053001, 2022.

Y. Yamanashi, *et al.*, *IEEE TAS* **23**, 1701004, 2013, 2013.

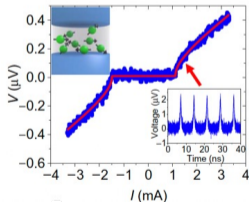
Artificial Synapses with Magnetic JJs

NIST

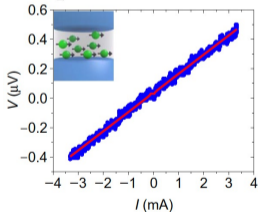
- Using Josephson junctions with magnetic nanoclusters
 - **Ultra-low energy:** spiking energy ~ 1 aJ (vs. ~ 10 fJ in human brain)
 - **Ultra-high density:** JJ size down to ~ 100 nm.

I-V characteristic of a 10- μm JJ synapse at 4 K

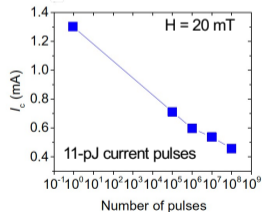
Disordered state



Ordered state



I_c as a function of ordering pulses

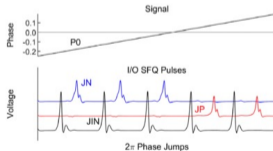
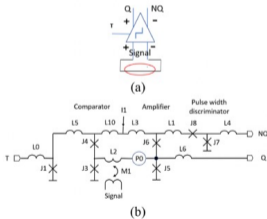


BioSFQ Circuits

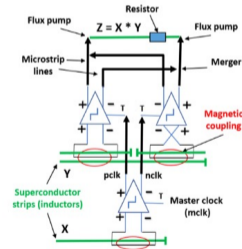
Stony Brook University, MIT Lincoln Laboratory

- Mixture of **analog and digital** circuits.
- Information is stored in a **SC loop** and transferred as a rate of SFQ pulses.

Analog comparator with complementary outputs



Bipolar analog multiplier

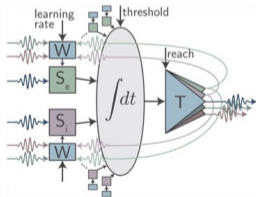


Superconducting Optoelectronic Neurons

NIST

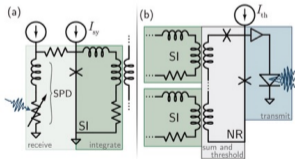
- **Communication:** Optical waveguides with LEDs and single-photon detectors (SPDs).
- **Computation:** Josephson circuits.

Optoelectronic neuron



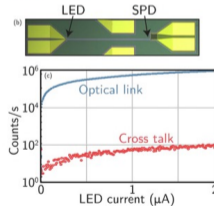
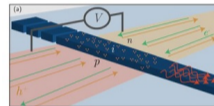
J. M. Shainline *et al.*, *J. Appl. Phys.* 126, 044902 (2019)

Superconducting synapse and neuron cell body



J. M. Shainline *et al.*, *J. Appl. Phys. Lett.* 118, 160501 (2021)

A silicon LED and waveguide coupled to a SPD



YNU YOKOHAMA National University

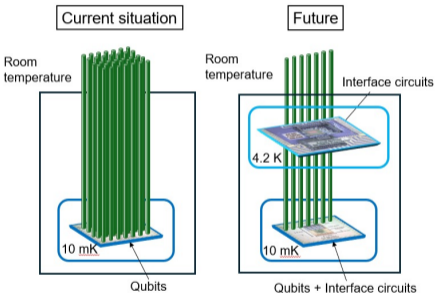
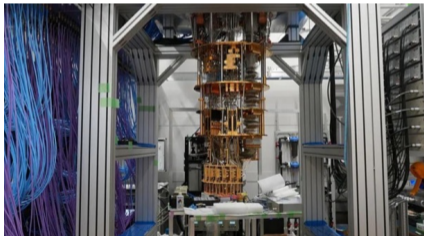
Comparison of Neuromorphic Circuits

	Biological (Brain)	Semiconductor (CMOS, memristor)	Superconductor (JJ, MJJ, SFQ)
Speed	~1 - 100s Hz (1 - 10 ms delay)	~1 - 100s MHz (~ 10 ns delay)	~10 - 100 GHz (~ 10 ps delay)
Energy/synapse	~ 10 fJ/synapse (20 W/brain)	~ pJ - 10s pJ	~ aJ or lower
Advantage	High density Massive parallelism High energy efficiency	room temp. operation Energy efficient than software Matured fab	Ultra fast Ultra low energy
Limitation	Slow	Power hungry	Cryogenic operation

Current Issue in SC Quantum Computers

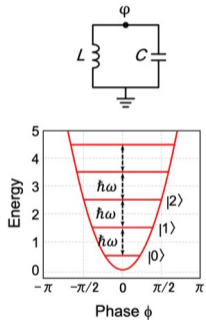
Each qubit requires 2-3 microwave lines between the mK stage and room temperature.

1000 qubits → ~2500 microwave lines

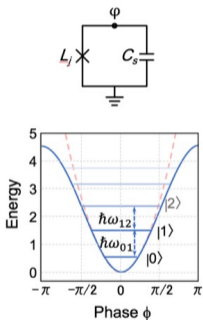


- Reduced wiring to room temperature
- High-speed qubit control

Superconducting Qubit

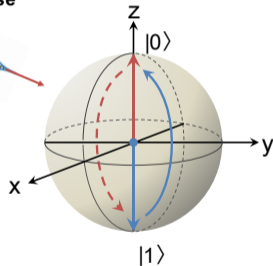
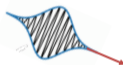


Quantum harmonic oscillator



Josephson qubit

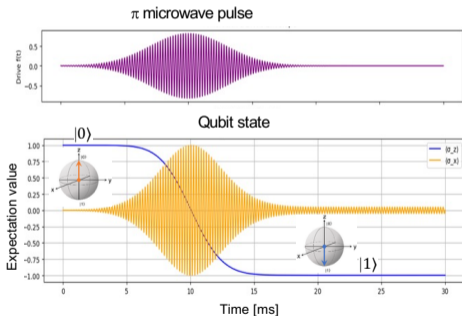
π -MW pulse



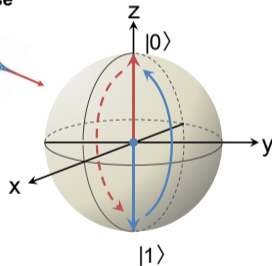
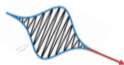
Bloch sphere and qubit states

Superconducting Qubit Irradiated with a π -MW Pulse

Qubit state control using a microwave pulse



π -MW pulse

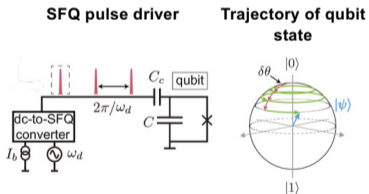


Bloch sphere and qubit states

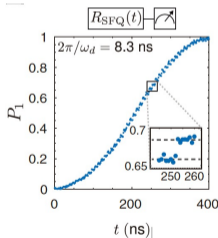
Digital Coherent Control of a Superconducting Qubit

University of Wisconsin-Madison, Syracuse University

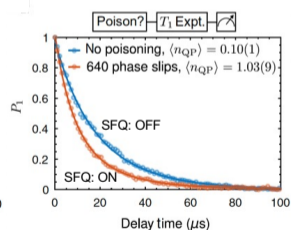
- An on-chip SFQ pulse driver integrated with a transmon qubit
- Average gate fidelity: **~95%**
- Coherence limited by **quasiparticle (QP) poisoning**



Qubit-state change driven by SFQ pulses



Energy decay curve w/o SFQ pulses



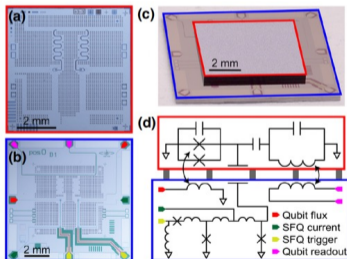
YNU YOKOHAMA National University

SFQ-Based Digital Qubit Control in an MCM

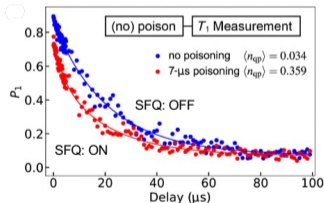
University of Wisconsin-Madison, Syracuse University, NIST, University of Colorado, LLNL

- SFQ driver and qubit on separate chips in a multichip module (MCM).
- Average gate fidelity: **98.8 %** (10 x improvement).
- Residual error arising from **photon-induced QP poisoning**.

Quantum-classical multichip module



Energy decay curve w/wo SFQ pulses

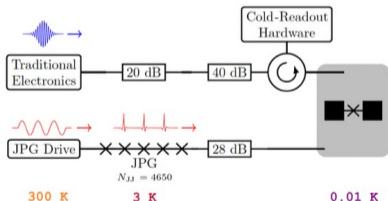


Qubit Control using a JJ Pulse Generator at 3 K

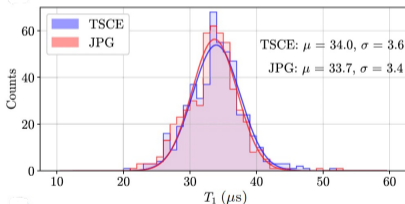
NIST, University of Colorado

- Transmon qubit controlled by Josephson pulse generator (JPG) at 3 K stage.
- Qubit lifetime T_1 comparable to room-temperature electronics.

Experimental setup



Histograms of qubit lifetime T_1 measured using JPG and RT electronics



Qubit lifetime

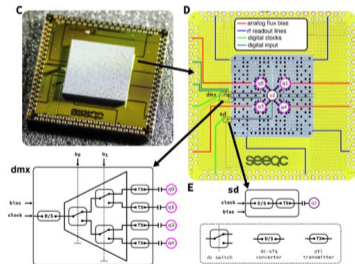
YNU YOKOHAMA National University

Multi-Qubit Control with SC Electronics at mK

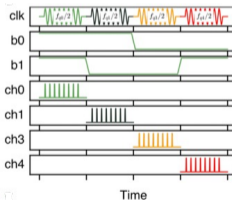
Seeqc, Inc.

- Implement **digital SFQ demultiplexer** with a multi-qubit system.
- Average gate fidelities: $\sim 99.5\%$ ■ Power dissipation for 1-4 DMX: **9 nW**

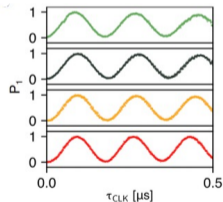
MCM composed of quantum & SFQ chips



Timing diagram of time-multiplexed qubit control



Time-multiplexed Rabi oscillations of the 4 qubits

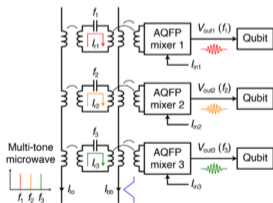


AQFP-Multiplexer for Qubit Control

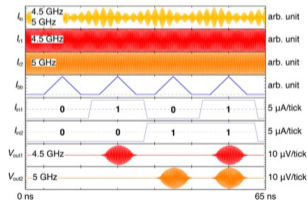
AIST, Tohoku University, NEC, Yokohama National University

- Multi-tone microwaves are multiplexed using AQFP gates
- Ultra-low-power qubit control: **81.8 pW per qubit**

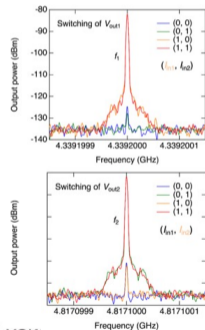
Block diagram of AQFP multiplexer



Simulated waveforms of AQFP multiplexer



Measured results at 4.2K



Comparison of Control Schemes for SC Qubits

	Room-Temp. Electronics	Cryo-CMOS	Superconducting Digital
Operating temp.	~ 300 K	3 – 4 K	10 -20 mK
Latency	High (cable delay) ~ 100 ns	Medium ~ 10 ns	Ultra-low ~ 100 ps
Power dissipation pre qubit	~10 mW – ~100 mW	~1 μ W – ~10 mW	~10 pW – ~10 nW
Thermal load	Heat from many cables and attenuators	~100 mW at 4 K	~10 μ W at 20 mK
Scalability	Limited by wiring	Reduce wires between 300K-4K	High scalability
Advantages	Mature & flexible	Fewer cables	Ultra-fast, ultra-low energy
Challenges	Latency & wiring bottlenecks	Power dissipation at low temp.	Integration density

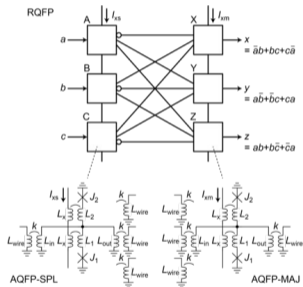
Reversible Computing

- In computation that **conserve information entropy**, there is **no fundamental lower limit** on the energy per bit.
- Landauer's principle sets a **$(k_B T \ln 2)$ limit only** when information is erased.
- Requirement to conserve information entropy :
 - Logical reversibility
 - Physical (thermodynamical) reversibility



Reversible AQFP (RQFP) Logic

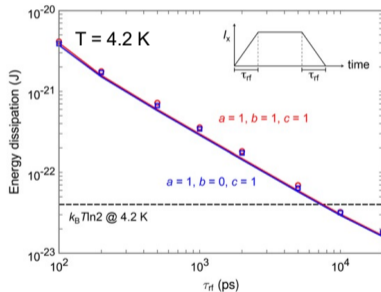
Reversible majority AQFP gate



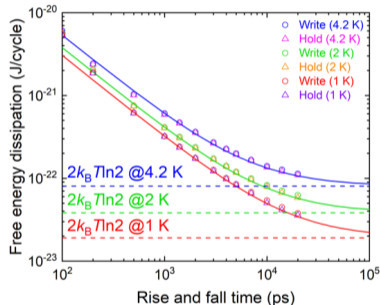
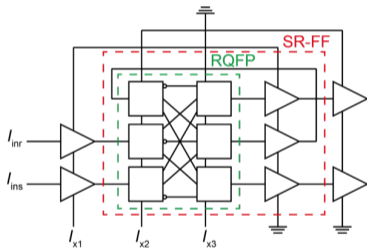
A logically and physically reversible gate can be realized by AQFP.

N. Takeuchi, et. al., *Scientific Reports* 4, 6354 (2014).

Simulated energy dissipation vs. rise time



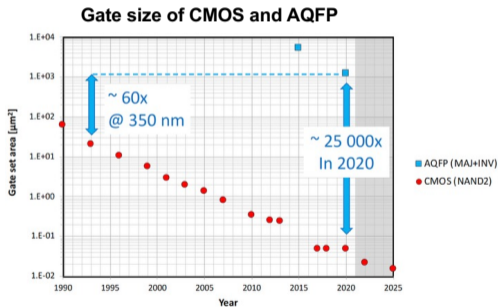
Energy Dissipation of an RQFP Flip-Flop



The energy dissipation of a reversible flip-flop approaches $2k_B T \ln 2$.
 ⇒ The energy dissipation is determined by data erasure.

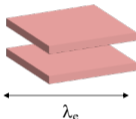
Challenge in Superconducting Digital Electronics

- Higher-density circuits and memories are needed



Fundamental Size of Charge- and Flux-Based Devices

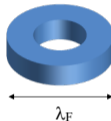
Charge-based



Energy to store
one electron

$$U_e = \frac{e^2}{2C} = \frac{e^2}{2\epsilon_0\lambda_e}$$

Flux-based



Energy to store
one SFQ

$$U_F = \frac{\Phi_0^2}{2L} = \frac{\Phi_0^2}{2\mu_0\lambda_F}$$

Equating energies ($U_e = U_F$), gives: $\frac{\lambda_F}{\lambda_e} = \left(\frac{\epsilon_0}{\mu_0}\right) \left(\frac{\Phi_0}{e}\right)^2 = 4 \left[\frac{h}{(2e)^2}\right]^2 / Z_0^2 = 4 \times \left(\frac{6.45\text{k}\Omega}{377\Omega}\right)^2 \sim 1000$

Quantum resistance

Space impedance

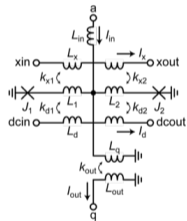
Flux-based devices are 1000 times larger than charge-based devices since quantum resistance is much larger than the space impedance.



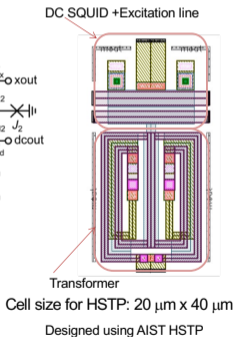
Use kinetic inductance to shrink flux-based devices.

Elimination of SC Transformer from AQFP

Schematic of AQFP buffer

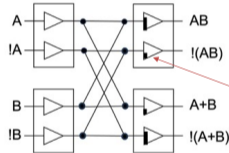


Layout of AQFP buffer

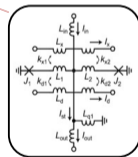


Dual-rail direct coupled AQFP (D²QFP) logic

D²QFP AND/OR gate

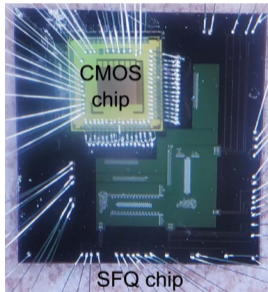


Total junction number: 16 JJ
cf: Conventional AQFP: 16 JJ



Other Activities for High-Density SC Digital Circuits

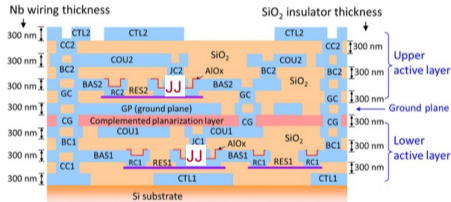
Josephson–CMOS Hybrid Memory



Readout operation at 38.4 Gb/s per channel was demonstrated.

Y. Hironaka *et al.*, *IEEE TAS* 35, 1300109, 2025

Double-Gate-Layered Niobium Process (DGP)



3D integration will be possible to implement.

T. Ando *et al.*, *Supercond. Sci. Technol.* 30, 075003, 2017.

Beginning of a New Era in SDE

■ Ultra-efficient AI

- Zero static loss and ultra-low switching energy
- Adiabatic and event-driven logic → much lower-power training and inference

■ Large-scale quantum computing

- Cryogenic control/readout with minimal heat near qubits
- Picosecond timing and low-noise amplifiers → high-fidelity quantum gates

■ Green computing

- Lower energy consumption and cooling loads
- “Cold accelerator” modules co-packaged with CMOS and photonics

■ What is needed next

- Higher-density circuits and memories
- Standardized PDKs and EDA workflows